

Dirac comb and exponential frequency spectra in nonlinear dynamics

Audun Theodorsen,^{1, a)} Gregor Decristoforo,¹ and Odd Erik Garcia¹

*Department of Physics and Technology, UiT The Arctic University of Norway,
N-9037 Tromsø, Norway*

(Dated: 2 November 2021)

An exponential frequency power spectral density is a well known property of many continuous time chaotic systems and has been attributed to the presence of Lorentzian-shaped pulses in the time series of the dynamical variables. Here a stochastic modelling of such fluctuations are presented, describing these as a superposition of pulses with fixed shape and constant duration. Closed form expressions are derived for the lowest order moments, auto-correlation function and frequency power spectral density in the case of periodic pulse arrivals and a random distribution of pulse amplitudes. In general, the spectrum is a Dirac comb located at multiples of the periodicity time and modulated by the pulse spectrum. Of the effects considered, only deviations from periodicity remove the Dirac Comb, and do so rapidly. Randomness in the pulse arrival times is investigated by numerical realizations of the process and the results are discussed in the context of the Lorenz system.

^{a)}Electronic mail: audun.theodorsen@uit.no

I. INTRODUCTION

Exponential frequency power spectra of fluctuation time series appears to be an intrinsic property of deterministic chaos in continuous time systems.¹⁻¹⁰ This has been observed in numerous experiments and model simulations of fluids and magnetized plasmas.¹⁻²⁷ Recently, the exponential spectrum has been attributed to the presence of Lorentzian pulses in the temporal dynamics.¹¹⁻²¹ Weakly non-linear systems are often characterized by quasi-periodic oscillations, resulting in a frequency power spectral density resembling a Dirac comb.¹⁹⁻²⁷ Far from the linear instability threshold the spectral peaks broaden and in many cases an exponential spectrum results.¹⁻²⁷

Many chaotic systems, including the Lorenz and the Rössler models, display quasi-periodic orbits with Lorentzian-shaped pulses close to the primary instability threshold. The associated PSD has sharp peaks at frequencies corresponding to the periodicity of the oscillations, resembling a Dirac comb. The Lorentzian-shaped pulses lead to an exponential modulation of the amplitude of these spectral peaks. With period-doubling the density of spectral peaks increases and in the chaotic state the spectral peaks broaden and the PSD eventually becomes an exponential function of frequency. It is of interest to note that exponential frequency spectra has also been reported from turbulent fluids and plasmas.^{17,18}

In this contribution, we present a stochastic model that describes the fluctuations as a super-position of Lorentzian pulses with fixed duration but an arbitrary distribution of pulse amplitudes and arrival times.²⁸⁻³⁰ The model is based on the process known as shot noise or filtered Poisson process (FPP), in which the uncorrelated pulses have a uniform distribution of arrival times and an exponential waiting time distribution.³²⁻⁴² In many cases, the FPP model allows analytical calculation of the fluctuation statistics such as auto-correlation function, probability density function and rate of level crossings in closed form. The FPP model has recently been used to describe intermittent fluctuations in turbulent fluids and plasmas.^{17,18} Here the stochastic model is generalized to an arbitrary distribution of pulse arrivals and the case of periodic pulse arrivals is considered in detail.

For a super-position of pulses with fixed shape and constant duration closed form expressions are here derived for the lowest order moments, auto-correlation function and frequency power spectral density in the case of periodic pulse arrivals and a random distribution of pulse amplitudes. In general, the spectrum is a Dirac comb located at multiples of the peri-

odicity time and modulated by the pulse spectrum. Randomness in the pulse arrival times is investigated by numerical realizations of the process and the results are discussed in the context of the Lorenz system. It is found that the stochastic model provides an excellent description of the fluctuation statistics for the chaotic dynamics.

The contribution is structured as follows. In Sec. II, a motivating example for studying periodic pulse trains in connection to chaotic motion is presented. In Sec. III the stochastic model for a super-position of pulses is presented and its PSD for general arrival times is derived. In Sec. IV the case of periodic pulse arrivals is analyzed in detail with a particular focus on Lorentzian pulses. Finally, in Sec. VI it is demonstrated that the stochastic model describes the chaotic dynamics of the Lorenz system.

II. THE LORENZ SYSTEM

A canonical chaos system is given by the Lorenz equations describing weakly non-linear thermal convection in an inversely stratified fluid,^{43–45}

$$\frac{dx}{dt} = \sigma(y - x), \quad (1)$$

$$\frac{dy}{dt} = x(\rho - z) - y, \quad (2)$$

$$\frac{dz}{dt} = xy - \beta z. \quad (3)$$

Here x , y and z are the dynamical variables and σ , ρ and β are the model parameters. In the following, we will normalize all time series according to

$$\tilde{z} = \frac{z - \langle z \rangle}{z_{\text{rms}}} \quad (4)$$

where $\langle z \rangle$ and z_{rms} are the time average and standard deviation, respectively.

The frequency PSD of the z -variable is presented in Fig. 1 for $\sigma = 10$, $\beta = 8/3$ and three different values of the model parameter ρ . For $\rho = 350$ the solution consists of nearly periodic oscillations and the frequency PSD resembles a Dirac comb with an exponential modulation of the peak amplitudes. As shown in Fig. 2, the oscillations are well described by periodically arriving Lorentzian-shaped pulses (see Appendix D for details). Following a period doubling bifurcation, the solution for $\rho = 220$ is still regular and the PSD is again dominated by a Dirac-like comb. For $\rho = 28$ the solution is chaotic and the PSD has an exponential shape for high frequencies and some narrow peaks for low frequencies. An excerpt of the time

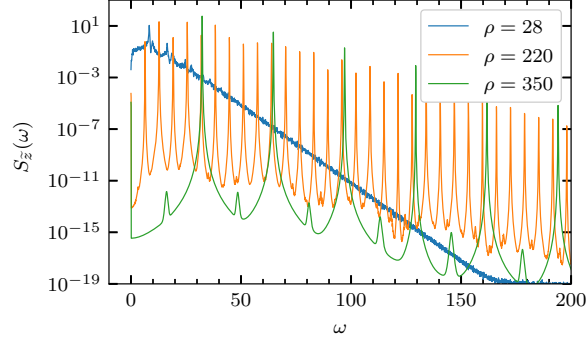


FIG. 1. Power spectral density of the normalized z -variable in the Lorenz system for $\sigma = 10$, $\beta = 8/3$ and various values of ρ .

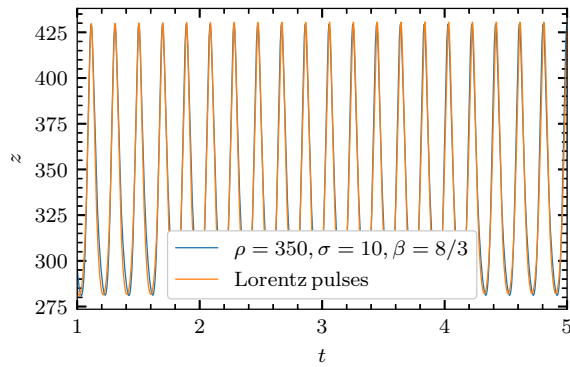


FIG. 2. Excerpt of the time series of the z -variable in the Lorenz system for $\sigma = 10$, $\beta = 8/3$ and $\rho = 350$ compared to a superposition of Lorentz pulses.

series is presented in Fig. 3. In the following, these features of the chaotic dynamics will be analyzed by describing the fluctuations as a super-position of Lorentzian-shaped pulses.

III. THE POWER SPECTRAL DENSITY OF A SUM OF PULSES

In this section, we develop an expression for the power spectral density of a process consisting of randomly (or periodically) arriving, superposed pulses. This is based on the formalism developed for filtered Poisson processes, also called the shot noise processes.

We consider a train of $K(T)$ pulses arriving in the interval $[-T/2, T/2]$ with randomly distributed arrival times $\{t_k\}_{k=1}^{K(T)}$ and randomly distributed amplitudes $\{A_k\}_{k=1}^{K(T)}$. The pulses have a characteristic shape φ and a characteristic duration time τ_d . K only depends on the

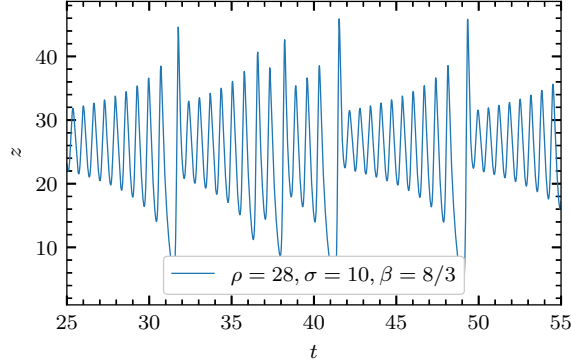


FIG. 3. Excerpt of the time series of the z -variable in the Lorenz system for $\sigma = 10$, $\beta = 8/3$ and $\rho = 28$.

time length T of the interval, not the value of the starting time.

Following these remarks, the process is written as a convolution between a pulse train f_K and a pulse shape φ :

$$\Phi_K(t) = \int_{-\infty}^{\infty} ds \varphi\left(\frac{t}{\tau_d} - s\right) f_K(s), \quad (5)$$

where

$$f_K(s) = \sum_{k=1}^{K(T)} A_k \delta\left(s - \frac{t_k}{\tau_d}\right) \quad (6)$$

and δ denotes the Dirac delta function. This can be viewed as a point process f_K passed through a filter with response function ϕ , hence the name. Note that for i.i.d. uniform pulse arrivals, $K(T)$ is a Poisson process.

We normalize the pulse shape such that

$$\int_{-\infty}^{\infty} |\varphi(s)| ds = 1. \quad (7)$$

We also introduce the notation

$$\rho_\varphi(s) = \frac{1}{I_2} \int_{-\infty}^{\infty} du \varphi(u) \varphi(u + s) \quad (8)$$

and

$$\varrho_\varphi(\theta) = \frac{1}{I_2} |\mathcal{F}[\varphi](\theta)|^2 \quad (9)$$

for the auto-correlation and the power spectral density of the pulse shape, respectively. Here,

$$I_n = \int_{-\infty}^{\infty} \varphi(s)^n ds. \quad (10)$$

Note that the functions ρ_φ and ϱ_φ form a Fourier transform pair, where the definition of the Fourier transform is given in Appendix A. Throughout this contribution, we will use Lorentzian pulses, which are detailed in Appendix D.

To find the PSD, we start from Eq. (5), and take the finite-time Fourier transform as defined in Appendix A:

$$\mathcal{F}_T[\Phi_K](\omega) = \int_{-T/2}^{T/2} dt \exp(-i\omega t) \Phi_K(t) = \int_{-T/2}^{T/2} dt \exp(-i\omega t) \int_{-\infty}^{\infty} ds \varphi(s) f_K\left(\frac{t}{\tau_d} - s\right) \quad (11)$$

where we have exchanged the functions in the convolution given by Eq. (5). A change of variables $u(t) = t - \tau_d s$ gives

$$\mathcal{F}_T[\Phi_K](\omega) = \int_{-\infty}^{\infty} ds \varphi(s) \exp(-i\tau_d \omega s) \int_{-T/2 - \tau_d s}^{T/2 - \tau_d s} du f_K\left(\frac{u}{\tau_d}\right) \exp(-i\omega u). \quad (12)$$

We assume that $\varphi(s)$ is negligible after a few τ_d . Moreover, since no pulses arrive for negative times, $f_K(u) = 0$ for $u < 0$. Assuming $T/\tau_d \gg 1$, we can therefore approximate the limits of the second integral in Eq. (12) as $u \in [-T/2, T/2]$, and the two integrals become independent. This gives

$$\mathcal{F}_T[\Phi_K](\omega) = \mathcal{F}[\varphi](\tau_d \omega) \mathcal{F}_T[f_K](\omega). \quad (13)$$

The power spectral density (PSD) of the stationary process Φ is therefore

$$\mathcal{S}_\Phi(\omega) = \lim_{T \rightarrow \infty} \frac{1}{T} \langle |\mathcal{F}_T[\Phi_K](\omega)|^2 \rangle = |\mathcal{F}[\varphi](\tau_d \omega)|^2 \lim_{T \rightarrow \infty} \frac{1}{T} \langle |\mathcal{F}_T[f_K](\omega)|^2 \rangle, \quad (14)$$

where $\mathcal{S}_\Phi(\omega)$ is independent of K , since the average is over all random variables. The power spectrum is thus the product of the power spectrum of the pulse shape and the power spectrum of the point process. Non-uniform arrivals only affect the point process, so this will be isolated in the analysis in Sec. III A.

Using Eq. (9), the full power spectral density of Φ can be written as

$$\mathcal{S}_\Phi(\omega) = I_2 \varrho_\varphi(\tau_d \omega) \lim_{T \rightarrow \infty} \frac{1}{T} \langle |\mathcal{F}_T[f_K](\omega)|^2 \rangle. \quad (15)$$

A. The power spectral density for general arrival times

The Fourier transform of the point process is

$$\mathcal{F}_T[f_K](\omega) = \tau_d \sum_{k=1}^K A_k \exp(-i\omega t_k). \quad (16)$$

Multiplying this expression with its complex conjugate and averaging over all random variables gives (for a general distribution of arrivals $P_{t_1, t_2, \dots, t_K}(t_1, t_2, \dots, t_K)$, assuming amplitudes are i.i.d. and independent of the arrival times):

$$\begin{aligned}
& \frac{1}{T} \langle |\mathcal{F}_T[f_K](\omega)^2| \rangle \\
&= \sum_{K=0}^{\infty} P_K(K; T, \tau_w) \frac{\tau_d^2}{T} \sum_{k=1}^K \sum_{l=1}^K \int_{-\infty}^{\infty} dt_1 \cdots \int_{-\infty}^{\infty} dt_K P_{t_1, \dots, t_K}(t_1, \dots, t_K) \\
&\quad \times \int_0^{\infty} dA_1 P_A(A_1) \cdots \int_0^{\infty} dA_K P_A(A_K) A_k A_l \exp(i\omega(t_l - t_k)). \\
&= \sum_{K=0}^{\infty} P_K(K; T, \tau_w) \frac{\tau_d^2}{T} \sum_{k, l=1}^K \langle A_k A_l \rangle \langle \exp(i\omega(t_l - t_k)) \rangle. \quad (17)
\end{aligned}$$

In this equation, there are K terms where $k = l$ and $K(K - 1)$ terms where $k \neq l$. Summing over all these terms, we have

$$\begin{aligned}
\frac{1}{T} \langle |\mathcal{F}_T[f_K](\omega)^2| \rangle &= \tau_d^2 \sum_{K=0}^{\infty} P_K(K; T, \tau_w) \\
&\quad \left\{ \frac{K}{T} \langle A^2 \rangle + \frac{1}{T} \langle A \rangle^2 \sum_{k=1}^K \sum_{l \neq k}^K \langle \exp(i\omega(t_l - t_k)) \rangle \right\}. \quad (18)
\end{aligned}$$

The average inside the exponential sum is the joint characteristic function of t_l and t_k . Exchanging the order of k and l in the double sum is the same as taking the complex conjugate of this characteristic function, so we get

$$\begin{aligned}
\frac{1}{T} \langle |\mathcal{F}_T[f_K](\omega)^2| \rangle &= \frac{\tau_d^2 \langle K \rangle}{T} \langle A^2 \rangle + \\
&\quad \frac{\tau_d^2}{T} \langle A \rangle^2 \sum_{K=0}^{\infty} P_K(K; T, \tau_w) \sum_{k=2}^K \sum_{l=1}^{k-1} 2\text{Re}[\langle \exp(i\omega(t_l - t_k)) \rangle]. \quad (19)
\end{aligned}$$

1. Uniformly distributed i.i.d arrivals

As an example, we show that the expression in Eq. (19) is consistent with the established result for $K(T)$ a pure Poisson point process.

Now t_l, t_k are i.i.d. uniformly distributed arrivals on $[0, T]$. We therefore have that

$$\langle \exp(i\omega(t_l - t_k)) \rangle = \langle \exp(i\omega t_l) \rangle \langle \exp(-i\omega t_k) \rangle = 2 \frac{1 - \cos(\omega T)}{\omega^2 T^2}. \quad (20)$$

All terms in the double sum are equal, and we get

$$\frac{1}{T} \langle |\mathcal{F}_T[f_K](\omega)^2| \rangle = \frac{\tau_d^2 \langle K \rangle}{T} \langle A^2 \rangle + 2 \frac{\tau_d^2}{T} \langle A \rangle^2 \langle K(K-1) \rangle \frac{1 - \cos(\omega T)}{\omega^2 T^2}. \quad (21)$$

In this case, K is Poisson distributed with mean and variance equal to T/τ_w and we get

$$\frac{1}{T} \langle |\mathcal{F}_T[f_K](\omega)^2| \rangle = \frac{\tau_d^2}{\tau_w} \langle A^2 \rangle + \frac{2\tau_d^2}{\tau_w^2} \langle A \rangle^2 T \frac{1 - \cos(\omega T)}{\omega^2 T^2}, \quad (22)$$

which gives, using $\gamma = \tau_d/\tau_w$ and that the last term contains $f_T(\omega)$ in Appendix F,

$$\lim_{T \rightarrow \infty} \frac{1}{T} \langle |\mathcal{F}_T[f_K](\omega)^2| \rangle = \tau_d \gamma \langle A^2 \rangle + 2\pi \tau_d \gamma^2 \langle A \rangle^2 \delta(\tau_d \omega). \quad (23)$$

This is the standard expression for the Poisson process⁴⁰. A Poisson process gives a flat spectrum, so the only frequency variation in the full spectrum will be due to the pulse function.

2. Periodic arrival times

We consider the situation where the periodicity is known, but the exact arrivals are not. This corresponds to uncertainty in where the measurement starts in relation to the first arrival time. If the arrivals are periodic, the marginal PDF of arrival k given that the starting time is s , is

$$P_{t_k|s}(t_k|s) = \delta(t_k - \tau_p k - s). \quad (24)$$

Since each arrival is deterministic, the joint PDF with known starting point is the product of the marginal PDFs, and we have

$$\langle \exp(i\omega(t_l - t_k)) \rangle = \exp(i\omega\tau_p(l - k)). \quad (25)$$

Note that this is independent of s for all starting points, so for now we need not consider s further. We have from Eq. (19)

$$\begin{aligned} \sum_{k=2}^K \sum_{l=1}^{k-1} 2\text{Re}[\langle \exp(i\omega(t_l - t_k)) \rangle] &= \sum_{k=2}^K \sum_{l=1}^{k-1} 2 \cos(\tau_p \omega(l - k)) \\ &= \frac{K - 1 + \cos(\tau_p \omega K) - K \cos(\tau_p \omega)}{\cos(\tau_p \omega) - 1} = \frac{\cos(\tau_p \omega K) - 1}{\cos(\tau_p \omega) - 1} - K. \end{aligned} \quad (26)$$

Due to the periodicity, there are $\lfloor T/\tau_p \rfloor$ events in a time series of length T . We use $P_K(K; T, \tau_p) = \delta(K - \lfloor T/\tau_p \rfloor)$. Inserting this and Eq. (26) into Eq. (19) gives

$$\frac{1}{T} \langle |\mathcal{F}_T[f_K](\omega)^2| \rangle = \frac{\tau_d^2}{T} \lfloor T/\tau_p \rfloor \langle A^2 \rangle + \frac{\tau_d^2}{T} \lfloor T/\tau_p \rfloor \langle A \rangle^2 \left[\lfloor T/\tau_p \rfloor^{-1} \frac{\cos(\tau_p \omega \lfloor T/\tau_p \rfloor) - 1}{\cos(\tau_p \omega) - 1} - 1 \right]. \quad (27)$$

For $T/\tau_p \gg 1$, $\lfloor T/\tau_p \rfloor/T \approx 1/\tau_p$, and we have (writing $K = \lfloor T/\tau_p \rfloor$)

$$\lim_{T \rightarrow \infty} \frac{1}{T} \langle |\mathcal{F}_T[f_K](\omega)^2| \rangle = \frac{\tau_d^2}{\tau_p} \langle A^2 \rangle - \frac{\tau_d^2}{\tau_p} \langle A \rangle^2 + \frac{\tau_d^2}{\tau_p} \langle A \rangle^2 \lim_{K \rightarrow \infty} \frac{1}{K} \frac{\cos(\tau_p \omega K) - 1}{\cos(\tau_p \omega) - 1}. \quad (28)$$

Let us consider the last part of the last term,

$$\lim_{K \rightarrow \infty} \frac{1}{K} \frac{\cos(\tau_p \omega K) - 1}{\cos(\tau_p \omega) - 1}. \quad (29)$$

For integer n and $\tau_p \omega \neq 2\pi n$, this limit is zero. For $\tau_p \omega \rightarrow 2\pi n$, this limit tends to ∞ . We might therefore consider Eq. (29) proportional to a train of δ -pulses located at $\tau_p \omega = 2\pi n$.

Setting $\tau_p \omega = 2\pi n + \epsilon$ where $\epsilon \ll 1$ and expanding the cosine in the denominator, we have

$$\lim_{K \rightarrow \infty} \frac{1}{K} \frac{\cos(\tau_p \omega K) - 1}{\cos(\tau_p \omega) - 1} \approx \lim_{K \rightarrow \infty} \frac{2}{K} \frac{1 - \cos(\epsilon K)}{\epsilon^2}. \quad (30)$$

This is on the same form as we had when deriving Eq. (23), so we conclude that

$$\lim_{K \rightarrow \infty} \frac{1}{K} \frac{\cos(\tau_p \omega K) - 1}{\cos(\tau_p \omega) - 1} \sim 2\pi \sum_{n=-\infty}^{\infty} \delta(\tau_p \omega - 2\pi n). \quad (31)$$

Inserting this into Eq. (27) gives the full expression for the PSD of a train of delta pulses with randomly distributed amplitudes:

$$\lim_{T \rightarrow \infty} \frac{1}{T} \langle |\mathcal{F}_T[f_K](\omega)^2| \rangle = \tau_d \gamma A_{\text{rms}}^2 + 2\pi \tau_d \gamma^2 \langle A \rangle^2 \sum_{n=-\infty}^{\infty} \delta(\tau_d \omega - 2\pi n \gamma). \quad (32)$$

This equation will be discussed in the following section.

IV. THE STOCHASTIC PROCESS WITH PERIODIC ARRIVALS

The full power spectral density of Φ is given by multiplying Eq. (32) by the power spectrum of the pulse functions, Eq. (9), as given by Eq. (15):

$$\mathcal{S}_\Phi(\omega) = \tau_d \gamma A_{\text{rms}}^2 I_{2\varrho_\varphi}(\tau_d \omega) + 2\pi \tau_d \gamma^2 \langle A \rangle^2 I_{2\varrho_\varphi}(\tau_d \omega) \sum_{n=-\infty}^{\infty} \delta(\tau_d \omega - 2\pi n \gamma). \quad (33)$$

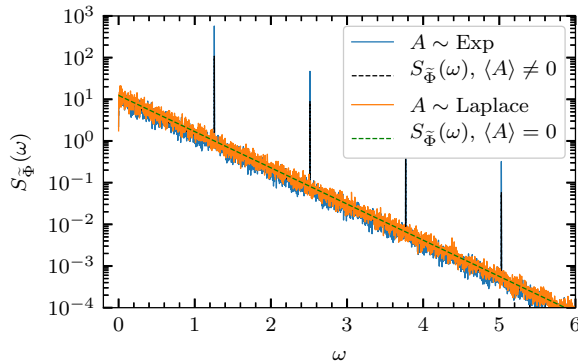


FIG. 4. The power spectral density of a shot noise process with periodic arrival times for exponentially (blue) and Laplace (orange) distributed amplitudes. The analytic expression is given by the black and green dashed lines, respectively.

There are two main differences from the uniformly distributed pulses, given by Eq. (23): A_{rms} enters into the first term instead of $\langle A^2 \rangle$, and there is a contribution of delta spikes at integer multiples of $2\pi/\tau_p$, with an envelope given by the pulse shape. We may view the first term as the average spectrum, due to the randomness of the amplitude distribution, while the second term containing the sum of delta pulses is due to the periodicity of the pulse arrivals. Accordingly, the first term vanishes for degenerately distributed amplitudes, $p_A(A) = \delta(A - \langle A \rangle)$. For a symmetric amplitude distribution around 0, $\langle A \rangle = 0$ and $A_{\text{rms}}^2 = \langle A^2 \rangle$. The periodicity is canceled out and only the first term remains.

In Fig. 4, the power spectral density of a synthetically generated shot noise is presented for exponentially distributed amplitudes (blue line) and symmetrically Laplace distributed amplitudes (orange line). The arrivals are periodic and the pulses have a Lorentzian shape. The analytic expression Eq. (33) for both cases is given by the black and green dashed lines respectively. The Dirac comb with decaying amplitudes is easily seen in the case with exponential amplitudes. We emphasize that the main effect of the periodicity, the Dirac comb, is completely cancelled out by the symmetrically distributed pulse amplitudes.

A. The correlation function

By the Wiener-Khinchin theorem,

$$R_{\Phi}(t) = \frac{1}{2\pi} \int_{-\infty}^{\infty} d\omega \mathcal{S}_{\Phi}(\omega) \exp(i\omega t) \quad (34)$$

$$= \gamma A_{\text{rms}}^2 I_2 \rho_{\varphi}(t/\tau_d) + \gamma^2 \langle A \rangle^2 I_2 \sum_{n=-\infty}^{\infty} \varrho_{\varphi}(2\pi n\gamma) \exp(i2\pi n\gamma t/\tau_d). \quad (35)$$

By using the Poisson summation formula and properties of the Fourier transform as detailed in Appendix C, we can write R_{Φ} as

$$R_{\Phi}(t) = \gamma A_{\text{rms}}^2 I_2 \rho_{\varphi}\left(\frac{t}{\tau_d}\right) + \gamma \langle A \rangle^2 I_2 \sum_{m=-\infty}^{\infty} \rho_{\varphi}\left(\frac{m}{\gamma} + \frac{t}{\tau_d}\right). \quad (36)$$

Writing $m/\gamma + t/\tau_d = (m + t/\tau_p)/\gamma$, we see that the correlation function consists of a central peak with followed by periodic modulations at integer multiples of τ_p . Again, for degenerate amplitudes the correlation function only consists of the periodic train: there is no randomness left in the signal and so the correlation function does not decay for large times. For symmetric amplitudes, only the central peak remains.

In Fig. 5, the auto-correlation function of a synthetically generated shot noise is presented for exponentially distributed amplitudes (blue line) and symmetrically Laplace distributed amplitudes (orange line). The arrivals are periodic and the pulses have a Lorentzian shape. The analytic expression Eq. (33) for both cases is given by the black and green dashed lines respectively. For exponentially distributed amplitudes, the periodicity is clearly seen. This effect is again completely cancelled out by symmetrically distributed amplitudes.

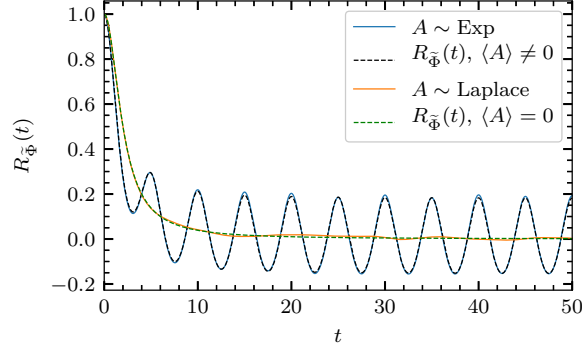


FIG. 5. The auto-correlation function of a shot noise process with periodic arrival times for exponentially (blue) and Laplace (orange) distributed amplitudes. The analytic expression is given by the black and green dashed lines, respectively.

B. The mean value and standard deviation

The mean value of the shot noise process with periodic pulses, assuming a uniform starting time distribution in $[0, \tau_p)$, is given by

$$\begin{aligned}
\langle \Phi_K \rangle &= \sum_{k=1}^K \int dA P_A(A) \int ds P_s(s) A \varphi\left(\frac{t - \tau_p k - s}{\tau_d}\right) \\
&= \frac{\langle A \rangle}{\tau_p} \sum_{k=1}^K \int_0^{\tau_p} ds \varphi\left(\frac{t - \tau_p k - s}{\tau_d}\right) \\
&= \frac{\langle A \rangle}{\tau_p} \sum_{k=1}^K \int_{(t - \tau_p(k+1))/\tau_d}^{(t - \tau_p k)/\tau_d} \tau_d du \varphi(u) = \gamma \langle A \rangle \int_{(t - (K+1)\tau_p)/\tau_d}^{(t - \tau_p)/\tau_d} du \varphi(u) \\
\langle \Phi \rangle &= \lim_{T \rightarrow \infty} \sum_{K=1}^{\infty} p_K(K; \tau_w, T) \langle \Phi_K \rangle = \gamma \langle A \rangle I_1.
\end{aligned} \tag{37}$$

In the last step, we let $T \rightarrow \infty$ giving $K \rightarrow \infty$ and set the upper integration limit to ∞ to avoid the effect due to the signal starting at $t = 0$. This is the expected result from Campbell's theorem. This is also consistent with the fact that the square mean value is given by the zero-frequency delta function in the power spectrum, $\mathcal{S}_{\Phi}(\omega) = 2\pi \langle \Phi \rangle^2 \delta(\omega) + \dots$

The second moment is most conveniently found by noting that

$$\langle \Phi \rangle^2 = \langle \Phi(t) \Phi(t) \rangle = R_{\Phi}(0) = \gamma A_{\text{rms}}^2 I_2 + \gamma \langle A \rangle^2 I_2 \sum_{m=-\infty}^{\infty} \rho_{\varphi}\left(\frac{m}{\gamma}\right), \tag{38}$$

where we have used that $\rho_\varphi(0) = 1$. This can be verified by calculating the second moment directly as was done for the first. In Appendix B, it is shown that this is also equivalent to an extension of Campbell's theorem. We get the variance

$$\Phi_{\text{rms}}^2 = \gamma A_{\text{rms}}^2 I_2 + \gamma \langle A \rangle^2 I_2 \left(\sum_{m=-\infty}^{\infty} \rho_\varphi(m/\gamma) - \gamma \frac{I_1^2}{I_2} \right). \quad (39)$$

In the case $\gamma \ll 1$, only the $m = 0$ term in the sum gives a contribution, $\rho_\varphi(0) = 1$, giving

$$\lim_{\gamma \rightarrow 0} \Phi_{\text{rms}}^2 = \gamma \langle A^2 \rangle I_2, \quad (40)$$

where we neglect the γ^2 -contribution of the last term in the bracket. Thus, in the limit of no pulse overlap, the variance for the case of periodic pulses is equivalent to the case of Poisson distributed pulses.

In the case $\gamma \gg 1$, we can write $m/\gamma = m\Delta_t \rightarrow t$ and treat the sum as an integral, $\gamma \sum_m \rho(m/\gamma)(1/\gamma) \approx \gamma \int \rho(t)\Delta_t = \gamma I_1^2/I_2$, where the sum is over all integers and the integral is over all reals. The terms inside the bracket cancel, and we get

$$\lim_{\gamma \rightarrow \infty} \Phi_{\text{rms}}^2 = \gamma A_{\text{rms}}^2 I_2. \quad (41)$$

Since $A_{\text{rms}}^2 = \langle A^2 \rangle - \langle A \rangle^2 \leq \langle A^2 \rangle$, the periodic pulse overlap gives lower variance than the Poisson distributed pulses as there is less randomness in the signal. For exponential amplitudes, the variance in the periodic case is a factor 2 smaller. For amplitudes with zero mean value, it is equal to the Poisson case while for fixed amplitudes, the signal has no variance as pulses will accumulate until the rate of accumulation exactly matches the rate of decay, after which the signal will remain constant.

V. DEVIATIONS FROM PERIODICITY

In this section, we will consider deviations from periodicity in a few different ways. It will be demonstrated that the Dirac comb is a very robust feature of the model as long as periodic arrivals are maintained. However, deviations from periodic arrivals very quickly remove most higher harmonics of the Dirac comb.

A. Quasi-periodic pulses

In this section, we present the effect of quasi-periodicity in the arrival time distribution on the second-order statistics of the stochastic process. Here, we model quasi-periodicity using a uniform distribution for each arrival around the periodic arrival time, so that the distribution of the k 'th arrival time given the starting time s is

$$P_{t_k}(t_k|s) = \begin{cases} \frac{1}{2\tau_p\kappa}, & -\tau_p\kappa \leq t_k - \tau_p k - s \leq \tau_p\kappa \\ 0, & \text{else} \end{cases}. \quad (42)$$

In the limit $\kappa \rightarrow 0$, we recover the periodic arrivals, while for $\kappa > 1$, the probability distributions of adjacent arrivals overlap. We emphasize that this is still a very restrictive formulation: even for $\kappa > 1$, each arrival is guaranteed to be centered on the time corresponding to the periodic arrival time, and the number of arrivals in a given interval is fixed up to end effects.

In Figs. 6 and 7, the effect of this quasi-periodicity is presented. The full lines give the power spectral densities and the auto-correlation functions of the shot noise process with quasi-periodic arrival times for different values of the κ -parameter, Lorentzian pulses and exponentially distributed amplitudes. The black dashed line gives the analytic prediction for purely periodic pulses. Even moderate deviations from pure periodicity quickly destroy the Dirac comb. For $\kappa = 1$, the spectrum and correlation function are already difficult to distinguish from the case of Poisson distributed arrivals. Thus, quasi-periodic phenomena in for example turbulent fluids cannot be expected to produce more than the first peak of the Dirac comb.

B. Multiple periodicities

In order to modelling period doubling, we now consider a situation where we have multiple periodicities, each with their own amplitudes and possible constant offsets. We then write the Fourier transform of the point process as

$$\mathcal{F}_T[f_K](\omega) = \tau_d \sum_{p=1}^P \sum_{k=1}^{K^p} A_k^p \exp(-i\omega[\tau^p k + \alpha^p]), \quad (43)$$

where τ^p are the periods, $\{A_k^p\}_{k=1}^{K^p}$ are the arrivals connected to the p 'th periodicity, α^p are constant offsets from the first periodicity so $\alpha^1 = 0$, and $K^p = \lfloor (T - \alpha^p)/\tau^p \rfloor$. We

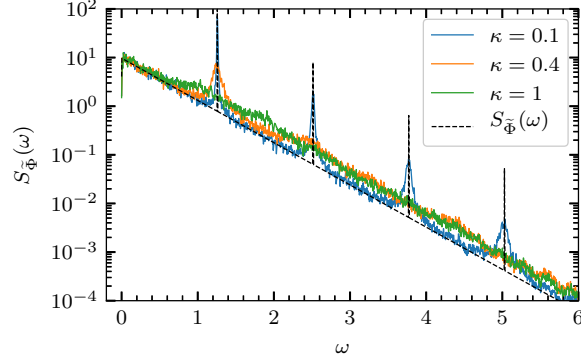


FIG. 6. The power spectral density of a shot noise process with quasi-periodic arrival times for different values of the κ -parameter. The analytic expression for purely periodic pulses is given by the black dashed line.

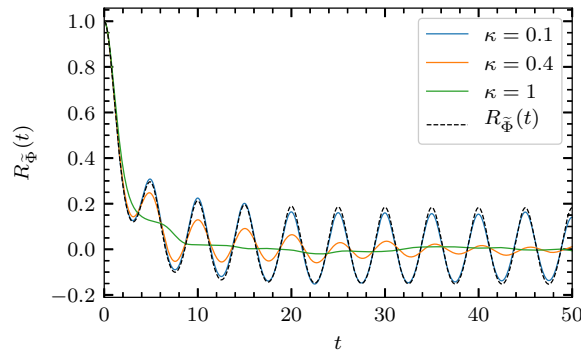


FIG. 7. The auto-correlation function of a shot noise process with quasi-periodic arrival times for different values of the κ -parameter. The analytic expression for purely periodic pulses is given by the black dashed line.

assume that the amplitudes for different periodicities are independent. Further, we arrange the periods in decreasing order, $\tau^1 \geq \tau^2 \geq \tau^3 \geq \dots$. For large enough T that the offsets can be neglected, this leads to an increasing order in the number of events, $K^1 \leq K^2 \leq K^3 \leq \dots$.

We get

$$\frac{1}{T} \langle |\mathcal{F}_T[f_K](\omega)|^2 \rangle = \frac{\tau_d^2}{T} \sum_{p,q=1}^P \sum_{k=1}^{K^p} \sum_{l=1}^{K^q} \langle A_k^p A_l^q \rangle \exp(-i\omega[\tau^p k - \tau^q l + \alpha^p - \alpha^q])$$

As before, $K^p = \lfloor T/\tau^p \rfloor$. The average over the binary combinations of amplitudes is $\langle A^{p2} \rangle$ if $p = q$ and $k = l$, $\langle A^p \rangle^2$ if $p = q$ and $k \neq l$ and $\langle A^p \rangle \langle A^q \rangle$ if $p \neq q$. This can be compactly

written as $\langle A_k^p A_l^q \rangle = A_{\text{rms}}^{p2} \delta_{p,q} \delta_{k,l} + \langle A^p \rangle \langle A^q \rangle$, and we get

$$\begin{aligned} \frac{1}{T} \langle |\mathcal{F}_T[f_K](\omega)^2| \rangle &= \frac{\tau_d^2}{T} \sum_{p=1}^P K^p A_{\text{rms}}^{p2} \\ &+ \frac{\tau_d^2}{T} \sum_{p,q=1}^P \langle A^p \rangle \langle A^q \rangle \exp(-i\omega[\alpha^p - \alpha^q]) \sum_{k=1}^{K^p} \sum_{l=1}^{K^q} \exp(-i\omega[\tau^p k - \tau^q l]). \\ \lim_{T \rightarrow \infty} \frac{1}{T} \langle |\mathcal{F}_T[f_K](\omega)^2| \rangle &= \tau_d^2 \sum_{p=1}^P \frac{1}{\tau^p} A_{\text{rms}}^{p2} \\ &+ \lim_{T \rightarrow \infty} \frac{\tau_d^2}{T} \sum_{p,q=1}^P \langle A^p \rangle \langle A^q \rangle \exp(-i\omega[\alpha^p - \alpha^q]) \frac{e^{-i\omega\tau^p K^p} - 1}{1 - e^{i\omega\tau^p}} \frac{e^{i\omega\tau^q K^q} - 1}{1 - e^{-i\omega\tau^q}} \end{aligned}$$

The first term is completely analogous to the first term in (32), summed over all periods. To investigate the last term, we consider the special case where $\tau^p = \tau \forall p$ so $K^p = K \forall p$. Then we have that

$$\begin{aligned} \lim_{T \rightarrow \infty} \frac{1}{T} \langle |\mathcal{F}_T[f_K](\omega)^2| \rangle &= \frac{\tau_d^2}{\tau} \sum_{p=1}^P A_{\text{rms}}^{p2} \\ &+ \lim_{T \rightarrow \infty} \frac{\tau_d^2}{T} \sum_{p,q=1}^P \langle A^p \rangle \langle A^q \rangle \exp(-i\omega[\alpha^p - \alpha^q]) \frac{\cos(K\omega\tau) - 1}{\cos(\omega\tau) - 1}. \end{aligned}$$

This contains exactly the expression found in Eq. (III A 2), so we have that the full expression is

$$\begin{aligned} \lim_{T \rightarrow \infty} \frac{1}{T} \langle |\mathcal{F}_T[f_K](\omega)^2| \rangle &= \tau_d \gamma \sum_{p=1}^P A_{\text{rms}}^{p2} \\ &+ 2\pi\tau_d \gamma^2 \sum_{p,q=1}^P \langle A^p \rangle \langle A^q \rangle \exp(-i\omega[\alpha^p - \alpha^q]) \sum_{n=-\infty}^{\infty} \delta(\tau_d \omega - 2\pi n \gamma). \end{aligned}$$

Here, $\gamma = \tau_d/\tau$. Thus, we get the same expression as for only one periodicity, except that we make the replacements

$$\begin{aligned} A_{\text{rms}}^2 &\rightarrow \sum_{p=1}^P (A_{\text{rms}}^p)^2, \\ \langle A \rangle^2 &\rightarrow \sum_{p=1}^P \sum_{q=1}^P \langle A^p \rangle \langle A^q \rangle \exp(-i\omega(\alpha^p - \alpha^q)). \end{aligned}$$

In this case, the correction to the second term in the expression for the PSD depends on the offset between the different pulse trains.

In the trivial case of no offset, $\alpha^p - \alpha^q = 0$, we just get the double sum over all mean values of the amplitudes, since this just amounts to adding the different periodicities on top of each other.

If we have alternating positive and negative pulses, so that $P = 2$, $\langle A^1 \rangle = -\langle A^2 \rangle = -\langle A \rangle$, $\alpha^1 = 0$ and $\alpha^2 = \tau/2$, the second replacement becomes $2\langle A^1 \rangle^2 [1 + \cos(\pi n)]$ at the delta spikes. Thus, every second spike is cancelled out and the distance between delta spikes is twice the true periodicity in the signal.

Adding further pulses with the same periodicity may affect the density of the spikes in the Dirac comb, but not its presence. Note that for a long enough time series ($T \rightarrow \infty$), the Dirac comb is always present, no matter the number of periods in the signal (that is, as long as period doubling has not given way to chaos) It is only when $\tau_p > T$ that we may lose the Dirac comb. To see this, we start from Eq. (43) and consider a situation with P periodic pulse trains, all with a periodicity τP . They are equally spaced so that $\alpha^p = \tau(p-1)$, and we let T be just below the periodicity time, $T = \tau P - \epsilon$, $\epsilon > 0$. In this case we let $T \rightarrow \infty$ by letting $P \rightarrow \infty$, so our observed time series is always just too short to catch the periodicity. After a few calculations similar to the previous case, we arrive at

$$\begin{aligned} \lim_{T \rightarrow \infty} \frac{1}{T} \langle |\mathcal{F}_T[f_K](\omega)^2| \rangle &= \tau_d \gamma \lim_{P \rightarrow \infty} \frac{1}{P} \sum_{p=1}^P A_{\text{rms}}^2 \\ &+ \tau_d \gamma \lim_{P \rightarrow \infty} \frac{1}{P} \sum_{p,q=1}^P \langle A^p \rangle \langle A^q \rangle \exp(-i\omega\tau[p-q]). \end{aligned}$$

Here $\gamma = \tau_d/\tau$ and we see that the infinite sums now play a role similar to sample averages. Further, the Dirac comb is potentially very easily recovered: for all integers n such that $\omega\tau = 2\pi n$, the exponential in the second term is 1, and the Dirac comb may exist if $\lim_{P \rightarrow \infty} (\sum_{p=1}^P \langle A^p \rangle)^2 / P$ diverges, and it is sufficient that for some a , $\langle A^p \rangle > a \forall p$. Intuitively, while this construction is strictly periodic with a periodicity larger than the observation time T , we recover the Dirac comb by viewing the amplitudes A^p as coming from one, more general amplitude distribution and this situation collapses to the single periodicity case with a different amplitude distribution. To avoid the Dirac comb, we require amplitudes that decay fast enough with the number of periodicities. Taking $\langle A^p \rangle = cp^\beta$, we have that the double sum at $\omega\tau = 2\pi n$ diverges for $\beta > -1/2$, converges to 4 for $\beta = 1/2$ and goes to zero for $\beta < -1/2$.

These discussions demonstrate that in general, it is very difficult to remove the Dirac comb

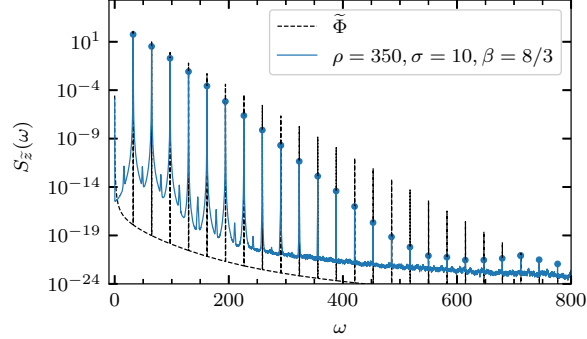


FIG. 8. The power spectral density of a Lorenz system with $\rho = 350$, $\sigma = 10$ and $\beta = 8/3$ compared to the frequency power spectral density of a synthetic shot noise process with periodic arrival times and exponentially distributed amplitudes. The local maxima of the power spectral density are indicated by blue dots.

while maintaining regularly spaced pulses. In Appendix H, we show that even allowing for a distribution of pulse shapes is not enough to avoid it. There is therefore only one effect left which consistently removes the Dirac comb, and that is deviations from periodicity in the time domain, as described in Sec. V A.

VI. APPLICATION TO THE LORENZ ATTRACTOR

The predictions for the PSD of the stochastic model can be compared to that from numerical simulations of Lorenz system. In Fig. 8 the low-frequency part of the spectrum is presented for $\rho = 350$ as well as the predicted Dirac comb for a super-position of Lorentzian pulses with duration $\tau_d = 0.039$ and periodicity $\tau_p = 0.194$. This is clearly a good description of the oscillations in the Lorenz system.

In the chaotic state for $\rho = 28$ the PSD presented in Fig. 9 has some low-frequency peaks with higher harmonics on top of a exponential spectrum. This spectrum can be reproduced by a super-position of quasi-periodic Lorentzian with duration $\tau_d = 0.135$, periodicity $\tau_p = 0.643$ and $\kappa = 0.1$ for the distribution of pulse arrivals. This is an excellent description of the PSD for the Lorenz system except for the very lowest frequencies which is likely due to deviations from the Lorentz pulse for very long times.

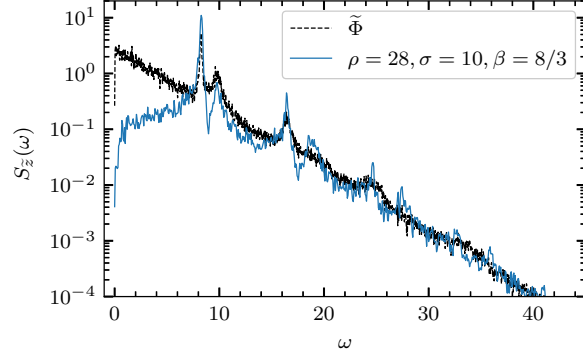


FIG. 9. The power spectral density of a Lorenz system with $\rho = 28$, $\sigma = 10$ and $\beta = 8/3$ compared to the power spectral density of a synthetic shot noise process with quasi-periodic arrival times, exponentially distributed amplitudes and $\kappa = 0.1$.

VII. APPLICATION TO THE VAN DER POL OSCILLATOR

To emphasize that the exponential modulation of the Dirac Comb is a consequence of nonlinear dynamics and not chaos, we here present frequency spectra for the Van der Pol oscillator^{46,47}:

$$\frac{d^2x}{dt^2} - \mu(1 - x^2)\frac{dx}{dt} + x = 0 \quad (44)$$

This model has a unique and stable limit cycle determined by the nonlinear damping parameter μ ⁴⁷. The frequency spectra are presented in Fig. ???. It is evident that the spectra are exponentially modulated.

VIII. DISCUSSION AND CONCLUSION

In this contribution, we have presented a formalism for describing the power spectra of time series from nonlinear dynamics as a superposition of pulses. The pulses may arrive periodically, appropriate for nonlinear oscillators, or according to a Poisson process, which is more appropriate for chaotic dynamics. Other arrival time distributions are also possible. For Poisson arrivals, the spectrum of the arrivals is flat while for periodic arrivals the spectrum is a Dirac comb. In both cases, the spectral decay is fully determined by the spectrum of the pulse shape which simply modulates the spectrum of the arrivals.

We have demonstrated that a Dirac comb with many higher harmonics is only present

for signals where the arrivals deviate very little from periodicity. Even for very modest deviations with all pulses either localized around the periodicity or for sharply unimodal waiting time distributions, we very quickly lose all higher harmonics except the first few. This demonstrates why spectra in even quasi-periodic chaos do not display a Dirac comb.

Lorenz pulses with fixed duration times have been shown to give a good description of the z-variable in the Lorentz system. The transition from periodic to chaotic is mainly due to deviations from the periodicity.

In the nonlinear Van der Pol oscillator, we see

We have demonstrated that exponential spectra are a feature of nonlinear oscillators in general and that chaos is not a necessary condition for exponential decay of the power spectral density.

IX. ACKNOWLEDGEMENTS

This work was supported by the UiT Aurora Centre Program, UiT The Arctic University of Norway (2020) and the Tromsø Research Foundation under grant number 19_SG_AT. Discussions with M. Rypdal and M. Overholt are gratefully acknowledged.

Appendix A: Definitions of the Fourier transform and the Power spectral density

The PSD of a random process $\Phi(t)$ is defined as

$$\mathcal{S}_\Phi(\omega) = \lim_{T \rightarrow \infty} \frac{1}{T} \langle |\mathcal{F}_T[\Phi](\omega)|^2 \rangle, \quad (\text{A1})$$

where

$$\mathcal{F}_T[\Phi_K](\omega) = \int_{-T/2}^{T/2} dt \exp(-i\omega t) \Phi(t) \quad (\text{A2})$$

is the finite-time Fourier transform of the random variable over the domain $[-T/2, T/2]$.

Analytical functions which fall rapidly enough to zero (such as the pulse function) have the Fourier transform

$$\mathcal{F}[\varphi](\theta) = \int_{-\infty}^{\infty} ds \varphi(s) \exp(-i\theta s) \quad (\text{A3})$$

and the inverse transform

$$\varphi(s) = \mathcal{F}^{-1}[\mathcal{F}[\varphi](\theta)](s) = \frac{1}{2\pi} \int_{-\infty}^{\infty} d\theta \exp(i\theta s) \mathcal{F}[\varphi](\theta). \quad (\text{A4})$$

Note that here, θ and s are non-dimensional variables, as opposed to t and ω .

Appendix B: The extended Campbell's theorem

For a full discussion of Campbell's theorem for the mean value of a shot noise process as well as various extentions, we refer to^{31,33,34}. It can be shown that for i.i.d. waiting times W with distribution p_W and mean value τ_w , we have in our notation

$$\begin{aligned} \langle \Phi^2 \rangle &= \gamma \langle A^2 \rangle I_2 + \\ &2\gamma \langle A \rangle^2 I_2 \sum_{k=1}^{\infty} \int_0^{\infty} ds_1 \int_0^{\infty} ds_2 \cdots \int_0^{\infty} ds_k p_W(s_1) p_W(s_2) \cdots p_W(s_k) \rho_{\varphi} \left(\frac{1}{\tau_d} \sum_{n=1}^k s_n \right). \end{aligned} \quad (\text{B1})$$

The k 'th order integral can be compactly written as $\langle \rho_{\phi}(S_k/\tau_d) \rangle$, where $S_k = \sum_{n=1}^k s_n$. All s_n are i.i.d., with distribution p_W , and we denote the corresponding characteristic function as C_W . We get

$$\left\langle \rho_{\varphi} \left(\frac{1}{\tau_d} S_k \right) \right\rangle = \int_{-\infty}^{\infty} dS p_S(S; k) \rho_{\varphi} \left(\frac{1}{\tau_d} S \right) = \frac{1}{2\pi} \int_{-\infty}^{\infty} du \int_{-\infty}^{\infty} dS C_S(u; k) \exp(-iSu) \rho_{\varphi} \left(\frac{1}{\tau_d} S \right). \quad (\text{B2})$$

As C_S is the characteristic function of the sum of k i.i.d. random variables, we get $C_S(u; k) = C_W(u)^k$. Further, we see that this equation contains the Fourier transform of ρ_{φ} , so we have

$$\left\langle \rho_{\varphi} \left(\frac{1}{\tau_d} S_k \right) \right\rangle = \frac{\tau_d}{2\pi} \int_{-\infty}^{\infty} du C_W(u)^k \varrho_{\varphi}(\tau_d u), \quad (\text{B3})$$

which gives

$$\langle \Phi^2 \rangle = \gamma \langle A^2 \rangle I_2 + 2\gamma \langle A \rangle^2 I_2 \sum_{k=1}^{\infty} \frac{\tau_d}{2\pi} \int_{-\infty}^{\infty} du C_W(u)^k \varrho_{\varphi}(\tau_d u). \quad (\text{B4})$$

For periodic arrivals, $p_W(w) = \delta(w - \tau_w)$, giving $C_W(u) = \exp(iu\tau_w)$, and we get

$$\langle \Phi^2 \rangle = \gamma \langle A^2 \rangle I_2 + 2\gamma \langle A \rangle^2 I_2 \sum_{k=1}^{\infty} \rho_{\varphi} \left(\frac{1}{\tau_d} k \tau_w \right). \quad (\text{B5})$$

As $A_{\text{rms}}^2 I_2 = \langle A^2 \rangle I_2 - \langle A \rangle^2 I_2 = \langle A^2 \rangle I_2 - \langle A \rangle^2 I_2 \rho_{\varphi}(0)$ and $\rho_{\varphi}(s) = \rho_{\varphi}(-s)$, this is equivalent to Eq. (38).

Appendix C: The Poisson summation formula

Here, we briefly present the well-known Poisson summation formula, which is treated in a number of textbooks^{48–51}. For our purposes, the formulation used in Corollary VII.2.6 in⁵¹ is the most useful. The statement in the book is for functions on general Euclidian spaces, but we repeat it here only for our special case (the real line):

The Poisson summation formula Suppose the Fourier transform of f and its inverse are defined as in Eq. (A3) and Eq. (A4) respectively. Further suppose that $|f(s)| \leq A(1 + |s|)^{-1-\delta}$ and $|\mathcal{F}[f](\theta)| \leq A(1 + |\theta/2\pi|)^{-1-\delta}$ with $A > 0$ and $\delta > 0$. Then

$$\sum_{m=-\infty}^{\infty} f(m) = \sum_{n=-\infty}^{\infty} \mathcal{F}[f](2\pi n), \quad (\text{C1})$$

where both series converge absolutely.

- Note that the inequality conditions guarantee that both $|f(s)|$ and $|\mathcal{F}[f](\theta)|$ are integrable, which again guarantees that both f and its Fourier transform are continuous and vanish at ∞ (Theorem I.1.2 in⁵¹).
- Using properties of the Fourier transform, the summation formula can be cast to a number of different forms:

$$\sum_{n=-\infty}^{\infty} \mathcal{F}[f](2\pi n) = \sum_{m=-\infty}^{\infty} f(m) \quad (\text{C2})$$

$$\sum_{n=-\infty}^{\infty} \gamma \mathcal{F}[f](2\pi n \gamma) = \sum_{m=-\infty}^{\infty} f(m/\gamma) \quad (\text{C3})$$

$$\sum_{n=-\infty}^{\infty} \gamma \mathcal{F}[f](2\pi n \gamma) \exp(i2\pi n \gamma t / \tau_d) = \sum_{m=-\infty}^{\infty} f(m/\gamma + t/\tau_d). \quad (\text{C4})$$

- By using the definitions of ρ and ϱ given in Eq. (8) and Eq. (9) respectively, as well as the Fourier transform, we have that if Eq. (C1) holds for φ , then by Eq. (C4) we have

$$\begin{aligned} \sum_{m=-\infty}^{\infty} \varphi(m+s) &= \sum_{n=-\infty}^{\infty} \mathcal{F}[\varphi](2\pi n) \exp(i2\pi n s), \\ \int_{-\infty}^{\infty} du \varphi(u) \sum_{m=-\infty}^{\infty} \varphi(s+m) &= \int_{-\infty}^{\infty} du \varphi(u) \sum_{m=-\infty}^{\infty} \mathcal{F}[\varphi](2\pi n) \exp(i2\pi n s), \\ \sum_{m=-\infty}^{\infty} \rho_{\varphi}(m) &= \sum_{n=-\infty}^{\infty} \varrho_{\varphi}(2\pi n), \end{aligned}$$

which means that the summation formula holds for the correlation function and power spectrum of the pulse as well. This does not necessarily work in reverse - if one of the sums over φ or its Fourier transform diverges, we cannot exchange the summation and the integral in the second step. Consider as an example the one-sided exponential pulse (detailed in Appendix E). Here, the pulse function does not fulfill the Poisson summation formula as the Fourier transform goes as θ^{-1} , and so the sum diverges. Its correlation function and power spectrum do, however, fulfill the conditions and therefore the formula.

Appendix D: The Lorentz pulse

The Lorentz pulse is given by

$$\varphi(s) = (1 + s^2)^{-1}/\pi. \quad (\text{D1})$$

Its Fourier transform is

$$\mathcal{F}[\varphi](\theta) = \exp(-|\theta|), \quad (\text{D2})$$

the integrals are³⁰

$$I_n = \frac{\Gamma(n - 1/2)}{\pi^{n-1/2}\Gamma(n)}, \quad (\text{D3})$$

and we have the correlation function

$$\rho_\varphi(s) = 4(4 + s^2)^{-1}, \quad (\text{D4})$$

and spectrum

$$\varrho_\varphi(\theta) = 2\pi \exp(-2|\theta|). \quad (\text{D5})$$

In general, the full sum of the correlation function is given by

$$\sum_{m=-\infty}^{\infty} \rho_\varphi\left(\frac{m}{\gamma} + \frac{t}{\tau_d}\right) = \gamma\pi[\coth(2\gamma\pi - i\gamma\pi t/\tau_d) + \coth(2\gamma\pi + i\gamma\pi t/\tau_d)]. \quad (\text{D6})$$

Two special cases of this are of interest in the current contribution. For $t = 0$, we get

$$\sum_{m=-\infty}^{\infty} \rho_\varphi\left(\frac{m}{\gamma}\right) = 2\gamma\pi \coth(2\gamma\pi), \quad (\text{D7})$$

while in the limit $\gamma \rightarrow 0$ we get the expected result

$$\lim_{\gamma \rightarrow 0} \sum_{m=-\infty}^{\infty} \rho_\varphi\left(\frac{m}{\gamma} + \frac{t}{\tau_d}\right) = \rho_\varphi(t/\tau_d). \quad (\text{D8})$$

Appendix E: Table of pulses

For reference, we here present some relations for other pulse functions.

Name	$\varphi(s)$	$\mathcal{F}[\varphi](\theta)$	$\rho_\varphi(s)$	$\varrho_\varphi(\theta)$
One-sided exponential	$\begin{cases} 0, & s < 0 \\ \exp(-s), & s \geq 0 \end{cases}$	$(1 + i\theta)^{-1}$	$\exp(- s)$	$2(1 + \theta^2)^{-1}$
Symmetric exponential	$\exp(- s)$	$2(1 + \theta^2)^{-1}$	$2\exp(- s)[1 + s]$	$8(1 + \theta^2)^{-2}$
Sech	$\text{sech}(s)/\pi$	$\text{sech}[\pi\theta/2]$	$s \text{csch}(s)$	$\pi^2 \text{sech}[\pi\theta/2]^2/2$
Gauss	$\exp(-s^2/2)/\sqrt{2\pi}$	$\exp(-\theta^2/2)$	$\exp(-s^2/4)$	$2\sqrt{\pi} \exp(-\theta^2)$

A few reasonable results for the infinite sums can be obtained:

Name	$\sum_{m=-\infty}^{\infty} \rho_\varphi(m/\gamma)$
One-sided exponential	$\coth\left(\frac{1}{2\gamma}\right)$
Symmetric exponential	$2 \coth\left(\frac{1}{2\gamma}\right) + \frac{1}{\gamma} \text{csch}\left(\frac{1}{2\gamma}\right)^2$

Appendix F: A representation of the Dirac delta function

A basic theorem in the theory of distributions is Theorem 2.5 in⁵²:

Let $f(x)$ be a piecewise continuous function such that $\int_{-\infty}^{\infty} |f(x)|dx < \infty$ and $\int_{-\infty}^{\infty} f(x)dx =$

1. Writing $f_a(x) = af(ax)$, we have that

$$f_a(x) \rightarrow \delta(x) \quad \text{as } a \rightarrow \infty. \quad (\text{F1})$$

In particular, we note that

$$f(x) = \frac{1 - \cos(x)}{\pi x^2} \quad (\text{F2})$$

fulfills the requirements of the theorem.

Appendix G: Representation of delta functions under finite sampling

In this contribution, we frequently plot delta functions superposed on a waveform. A true representation of a continuous-time delta function would be a line extending out of the plot domain. Alternatively, we could indicate the delta spikes by arrows or stars on the ends.

The first solution does not give an indication of the amplitude of the delta, while the second makes for very busy figures.

We have instead elected to represent the Dirac delta by its discrete analog, the Kronecker delta. For $t \rightarrow \Delta_t n$, we have $\omega = 2\pi f \rightarrow 2\pi m/\Delta_t$. A Dirac delta at a given angular frequency ω_* is then given by $\delta(\omega - \omega_*) = \delta(2\pi(m - k)/\Delta_t) = \frac{\Delta_t}{2\pi} \delta_{m-k}$ where k is the nearest integer to $\Delta_t \omega_*/2\pi$. That is, the Dirac delta is approximated as a boxcar of width equal to the sampling step and a height equal to the inverse of the sampling step. This indicates the amplitude of the delta spikes, separates them from any superposed functions and tends to better approximations for finer sampling.

Appendix H: Distribution of pulse shapes

In this appendix, we discuss the impact of allowing for variations in the pulse shape while maintaining the periodic arrivals. We do this by allowing the pulse duration time τ_d to be randomly distributed as well as allowing for other randomly distributed pulse parameters λ_k . In this case, we cannot separate the pulse train f_K from the rest of the time series, and we must express the process as

$$\Phi_K(t) = \sum_{k=1}^{K(T)} A_k \varphi\left(\frac{t - \tau_p k}{\tau_k}; \lambda_k\right)$$

Note that here, we have explicitly assumed periodic pulse arrivals.

The Fourier transform of this expression is

$$\begin{aligned} \mathcal{F}_T[\Phi_K](\omega) &= \int_0^T dt \exp(-i\omega t) \Phi_K(t) \\ &= \sum_{k=1}^{K(T)} A_k \exp(-i\omega \tau_p k) \int_{-\tau_p k/\tau_k}^{(T-\tau_p k)/\tau_k} dt \exp(-i\omega \tau_k s) \varphi(s; \lambda_k) \\ &\approx \sum_{k=1}^{K(T)} A_k \exp(-i\omega \tau_p k) \mathcal{F}[\varphi(s; \lambda_k)](\omega \tau_k), \end{aligned}$$

where we have discounted end effects in the integral. The full power spectral density is

therefore (where \dagger indicates the complex conjugate)

$$\begin{aligned}
\mathcal{S}_\Phi(\omega) &= \lim_{T \rightarrow \infty} \frac{1}{T} \sum_{k,l=1}^{K(T)} \langle A_k A_l \mathcal{F}[\varphi(s; \lambda_k)](\omega \tau_k) \mathcal{F}[\varphi(s; \lambda_k)](\omega \tau_k)^\dagger \rangle \exp(-i\omega \tau_p(k-l)) \\
&= \lim_{T \rightarrow \infty} \frac{1}{T} \sum_{k,l=1}^{K(T)} I_2 \langle A^2 \varrho_\varphi(\tau_k \omega; \lambda_k) \rangle \\
&\quad + \lim_{T \rightarrow \infty} \frac{1}{T} |\langle A \mathcal{F}[\varphi(s; \lambda)](\omega \tau) \rangle|^2 \sum_{k,l=1}^{K(T)} \exp(-i\omega \tau_p(k-l))
\end{aligned}$$

Here, we have explicitly assumed that the amplitudes, duration times and pulse parameters are independent of the arrival time. It is now clear that introducing randomness in the pulse duration or shape parameters only affects the modulation of the Dirac comb, not the existence of the comb itself.

REFERENCES

- ¹P. Atten, J. C. Lacroix, and B. Malraison, “Chaotic motion in a Coulomb force driven instability: large aspect ratio experiments” *Phys. Lett. A* **79**, 255 (1980).
- ²U. Frisch and R. Morf, “Intermittency in nonlinear dynamics and singularities at complex times” *Phys. Rev. A* **23**, 2673 (1981).
- ³H. S. Greenside, G. Ahlers, P. C. Hohenberg, and R. W. Walden, “A simple stochastic model for the onset of turbulence in Rayleigh-Bénard convection” *Physica D* **5**, 322 (1982).
- ⁴D. S. Broomhead and G. P. King, “Extracting qualitative dynamics from experimental data” *Physica* **10D**, 217 (1986).
- ⁵A. Brandstater and H. L. Swinney, “Strange attractors in weakly turbulent Couette-Taylor flow” *Phys. Lett. A* **35**, 2207 (1987).
- ⁶C. L. Streett and M. Y. Hussaini, “A numerical simulation of the appearance of chaos in finite-length Taylor-Couette flow” *Applied Numerical Mathematics* **7**, 41 (1991).
- ⁷D. E. Sigeiti, “Exponential decay of power spectra at high frequency and positive Lyapunov exponents” *Physica D* **82**, 136 (1995).
- ⁸D. E. Sigeiti, “Survival of deterministic dynamics in the presence of noise and the exponential decay of power spectra at high frequency” *Phys. Rev. E* **52**, 2443 (1995).
- ⁹M. R. Paul, M. C. Cross, P. F. Fischer, and H. S. Greenside, “Power-law behavior of power

- spectra in low Prandtl number Rayleigh-Bénard convection” *Phys. Rev. Lett.* **87**, 154501 (2001).
- ¹⁰C. L. E. Franzke, S. M. Osprey, P. Davini and N. W. Watkins, “A dynamical systems explanation of the Hurst effect and atmospheric low-frequency variability” *Sci. Rep.* **5**, 9068 (2015).
- ¹¹D. C. Pace, M. Shi, J. E. Maggs, G. J. Morales, and T. A. Carter, “Exponential frequency spectrum in magnetized plasmas” *Phys. Rev. Lett.* **101**, 085001 (2008).
- ¹²D. C. Pace, M. Shi, J. E. Maggs, G. J. Morales, and T. A. Carter, “Exponential frequency spectrum and Lorentzian pulses in magnetized plasmas” *Phys. Plasmas* **15**, 122304 (2008).
- ¹³G. Hornung, B. Nold, J. E. Maggs, G. J. Morales, M. Ramisch, and U. Stroth, “Observation of exponential spectra and Lorentzian pulses in the TJ-K stellarator” *Phys. Plasmas* **18**, 082303 (2011).
- ¹⁴J. E. Maggs and G. J. Morales, “Origin of Lorentzian pulses in deterministic chaos” *Phys. Rev. E* **86**, 015401 (2012).
- ¹⁵J. E. Maggs, T. L. Rhodes, and G. J. Morales, “Chaotic density fluctuations in L-mode plasmas of the DIII-D tokamak” *Plasma Phys. Contr. Fusion* **55**, 085014 (2013).
- ¹⁶Z. Zhu, A. E. White, T. A. Carter, S. G. Baek, and J. L. Terry, “Chaotic edge density fluctuations in the Alcator C-Mod tokamak” *Phys. Plasmas* **24**, 042301 (2017).
- ¹⁷G. Decristoforo, A. Theodorsen, and O. E. Garcia, “Intermittent fluctuations due to Lorentzian pulses in turbulent thermal convection” *Phys. Fluids* **32**, 085102 (2020).
- ¹⁸G. Decristoforo, A. Theodorsen, J. Omotani, T. Nicholas, and O. E. Garcia, “Intermittent fluctuations due to Lorentzian pulses in turbulent thermal convection” *Phys. Fluids* **32**, 085102 (2020).
- ¹⁹N. Ohtomo, K. Tokiwano, Y. Tanaka, A. Sumi, S. Terachi, and H. Konno, “Exponential characteristics of power spectral densities caused by chaotic phenomena” *J. Phys. Soc. Japan* **64**, 1104 (1995).
- ²⁰J. E. Maggs and G. J. Morales, “Generality of deterministic chaos, exponential spectra, and Lorentzian pulses in magnetically confined plasmas” *Phys. Rev. Lett.* **107**, 185003 (2011).
- ²¹J. E. Maggs and G. J. Morales, “Exponential power spectra, deterministic chaos and Lorentzian pulses in plasma edge dynamics” *Plasma Phys. Contr. Fusion* **54**, 124041 (2012).

- ²²J. D. Farmer, “Chaotic attractors of an infinite-dimensional dynamical system” *Physica D* **4**, 366 (1982).
- ²³A. Libchaber, S. Fauve, and C. Laroche, “Two-parameter study of the routes to chaos” *Physica D* **7**, 73 (1983).
- ²⁴E. F. Stone, “Power spectra of the stochastically forced Duffing oscillator” *Phys. Lett. A* **148**, 434 (1990).
- ²⁵T. Klinger, A. Latten, A. Piel, G. Bonhomme, T. Pierre, and T. Dudok de Wit, “Route to drift wave chaos and turbulence in a bounded low- β plasma experiment” *Phys. Rev. Lett.* **79**, 3913 (1997).
- ²⁶B. Mensour and A. Longtin, “Power spectra and dynamical invariants for delay-differential and difference equations” *Physica D* **113**, 1 (1998).
- ²⁷L. A. Safonov, E. Tomer, V. V. Strygin, Y. Ashkenazy, and S. Havlin, “Multifractal chaotic attractors in a system of delay-differential equations modeling road traffic” *Chaos* **12**, 1006 (2002).
- ²⁸O. E. Garcia and A. Theodorsen, “Power law spectra and intermittent fluctuations due to uncorrelated Lorentzian pulses” *Phys. Plasmas* **24**, 020704 (2017).
- ²⁹O. E. Garcia and A. Theodorsen, “Skewed Lorentzian pulses and exponential frequency power spectra” *Phys. Plasmas* **25**, 014503 (2018).
- ³⁰O. E. Garcia and A. Theodorsen, “Intermittent fluctuations due to uncorrelated Lorentzian pulses” *Phys. Plasmas* **25**, 014506 (2018).
- ³¹N. Campbell, *Proc. Cambridge Phil. Soc.* **15**, 117 (1909); **15** 310 (1909).
- ³²E. Parzen, *Stochastic processes* (Holden-Day, Oakland, CA, 1962).
- ³³H. L. Pécseli, *Fluctuations in Physical Systems* (Cambridge University Press, Cambridge, 2000).
- ³⁴S. O. Rice, “Mathematical analysis of random noise” *Bell Sys. Tech. J.* **23**, 282 (1944).
- ³⁵O. E. Garcia, “Stochastic modeling of intermittent scrape-off layer plasma fluctuations” *Phys. Rev. Lett.* **108**, 265001 (2012).
- ³⁶R. Kube and O. E. Garcia, “Convergence of statistical moments of particle density time series in scrape-off layer plasmas” *Phys. Plasmas* **22**, 012502 (2015).
- ³⁷A. Theodorsen and O. E. Garcia, “Level crossings, excess times, and transient plasma-wall interactions in fusion plasmas” *Phys. Plasmas* **23**, 040702 (2016).
- ³⁸O. E. Garcia, R. Kube, A. Theodorsen, and H. L. Pécseli, “Stochastic modelling of in-

- intermittent fluctuations in the scrape-off layer: Correlations, distributions, level crossings, and moment estimation” *Phys. Plasmas* **23**, 052308 (2016).
- ³⁹O. E. Garcia and A. Theodorsen, “Auto-correlation function and frequency spectrum due to a super-position of uncorrelated exponential pulses” *Phys. Plasmas* **24**, 032309 (2017).
- ⁴⁰A. Theodorsen, O. E. Garcia, and M. Rypdal, “Statistical properties of a filtered Poisson process with additive random noise: distributions, correlations and moment estimation” *Phys. Scripta* **92**, 054002 (2017).
- ⁴¹A. Theodorsen and O. E. Garcia, “Level crossings and excess times due to a superposition of uncorrelated exponential pulses” *Phys. Rev. E* **97**, 012110 (2018).
- ⁴²A. Theodorsen and O. E. Garcia, “Probability distribution functions for intermittent scrape-off layer plasma fluctuations” *Plasma Phys. Contr. Fusion* **60**, 034006 (2018)
- ⁴³E. N. Lorenz, “Deterministic nonperiodic flow” *J. Atmos. Sci.* **20**, 130 (1963)
- ⁴⁴K. Rypdal and O. E. Garcia, “Reduced Lorenz models for anomalous transport and profile resilience” *Phys. Plasmas* **14**, 022101 (2007).
- ⁴⁵O. E. Garcia, N. H. Bian, V. Naulin, A. H. Nielsen, and J. Juul Rasmussen “Two-dimensional convection and interchange motions in fluids and magnetized plasmas” *Phys. Scripta* **T122**, 104 (2006)
- ⁴⁶B. van der Pol, ”A theory of the amplitude of free and forced triode vibrations”, *Radio Review*, **1**, 701-710, 754-762 (1920).
- ⁴⁷S. H. Strogatz, ”Nonlinear Dynamics and Chaos” Perseus Books, New York, 1994
- ⁴⁸M. Overholt, A Course in Analytic Number Theory. American Mathematical Society (AMS) 2014 ISBN 978-1-4704-1706-2.
- ⁴⁹S. Bochner, Lectures on Fourier Integrals, Annals of Math. Studies 42, Princeton University press, Princeton, NJ, 1959
- ⁵⁰L. Grafakos, “Classical Fourier Analysis”, <https://doi.org/10.1007/978-0-387-09432-8>
- ⁵¹E. M. Stein and G. Weiss, “Introduction to Fourier Analysis on Euclidian Spaces”, Princeton University Press, Princeton, NJ, 1971
- ⁵²I. Richards and H. Youn, “Theory of Distributions”, Cambridge University Press, <https://doi.org/10.1017/CBO9780511623837>